Arabian Journal of Chemistry (2019) **12**, 1108–1120

King Saud University

**Arabian Journal of Chemistry**

www.ksu.edu.sa
www.sciencedirect.com

ORIGINAL ARTICLE

# *Ganoderma applanatum*-mediated green synthesis of silver nanoparticles: Structural characterization, and *in vitro* and *in vivo* biomedical and agrochemical properties

**Sudisha Jogaiah [a,*], Mahantesh Kurjogi [a], Mostafa Abdelrahman [b,c], Nagabhushana Hanumanthappa [d], Lam-Son Phan Tran [e,f,*]**

[a] *Plant Healthcare and Diagnostic Center, Department of Studies in Biotechnology and Microbiology, Karnatak University, Dharwad 580 003, India*
[b] *Graduate School of Life Science, Tohoku University, Sendai, Japan*
[c] *Department of Botany, Faculty of Science, Aswan University, Aswan, Egypt*
[d] *Department of Studies and Research in Physics, Tumkur University, Tumkur, India*
[e] *Institute of Research and Development, Duy Tan University, 03 Quang Trung, Da Nang, Viet Nam*
[f] *Signaling Pathway Research Unit, RIKEN Center for Sustainable Resource Science, 1-7-22 Suehiro-cho, Tsurmi-ku, Yokohama 230-0045, Japan*

Received 7 October 2017; accepted 2 December 2017
Available online 8 December 2017

**KEYWORDS**

Green synthesis;
Silver nanoparticles;
*Ganoderma applanatum*;
Antimicrobial;
Antioxidant

**Abstract** This study presents the use of basidiomycete extracts as an effective platform for "green synthesis" of silver nanoparticles (AgNPs). Out of seven basidiomycete species, *Ganoderma applanatum* displayed the highest antimicrobial properties against the tested pathogens. Thus, *G. applanatum* methanol crude extract was fractionated using column chromatography, and the obtained fractions were subjected to an antimicrobial assay followed by phytochemical analyses using high-performance liquid chromatography to select the best fraction for synthesis of AgNPs. Fraction 3 displayed potent antimicrobial activities as evidenced by its high phenolic content, and thus was used for AgNP biosynthesis. The *G. applanatum* fraction 3-synthesized AgNPs were then characterized using various microscopy, spectroscopy and X-ray diffraction techniques. The characteristic features

* Corresponding authors at: Plant Healthcare and Diagnostic Center, Department of Studies in Biotechnology and Microbiology, Karnatak University, India (S. Jogaiah) and Signaling Pathway Research Unit, RIKEN Center for Sustainable Resource Science, 1-7-22 Suehiro-cho, Tsurmi-ku, Yokohama 230-0045, Japan (L.-S.P. Tran).
E-mail addresses: jsudish@kud.ac.in (S. Jogaiah), mahantesh.kurjogi@gmail.com (M. Kurjogi), meettoo2000@ige.tohoku.ac.jp (M. Abdelrahman), bhushanvlc@gmail.com (N. Hanumanthappa), son.tran@riken.jp (L.-S.P Tran).
Peer review under responsibility of King Saud University.

Production and hosting by Elsevier

https://doi.org/10.1016/j.arabjc.2017.12.002

of the synthesized AgNPs indicated the spherical shape of AgNPs with an average size of 20–25 nm. The synthesized AgNPs exhibit high antioxidant capacity, *in vitro* antibacterial activity against *Staphylococcus aureus* and *Escherichia coli*, and *in vivo* antifungal properties against *Botrytis cinerea* and *Colletotrichum gloeosporioides* in tomato and strawberry leaflet assays, respectively. Our results demonstrated that *G. applanatum* can be efficiently used in synthesis of AgNPs with potent antimicrobial properties, which can be used for both clinical and agrochemical purposes.



## 1. Introduction

Microbial infection is a serious problem in agriculture and healthcare sector worldwide. Therefore, it is imperative to develop novel antimicrobial agents with versatile characteristics, such as antimicrobial potency, low toxicity and great compatibility. In this context, nanoparticles (NPs) have garnered worldwide interest, due to their electrostatic attraction between positively charged NPs and negatively charged microbial cells, and a large surface to volume ratio, resulting in improved physicochemical properties and enhanced antimicrobial activities of the NPs (Lakshmeesha et al., 2014; Kavyashree et al., 2015). The antimicrobial properties of NPs, including antibacterial and antifungal activities, have recently been widely reported (Mallmann et al., 2015; Salem et al., 2015; Elgorban et al., 2016). The novel properties of NPs make them extremely versatile in many areas of research like biomedical sciences, drug discovery, luminescence, cosmetics and renewable energy technologies (Chaudhuri and Paria, 2012; Tran et al., 2013; Rauwel et al., 2015). Silver NPs (AgNPs) are among the most important NPs with global scientific attention due to their unique properties, including potent antimicrobial activities, chemical stability, and high thermal and electrical conductivity (Tran et al., 2013; Yang et al., 2015; Quester et al., 2016). These properties enable promotion of AgNP applications as an antimicrobial agent in different arrays of products, such as soaps, plastics, food and textiles, increasing their market value (Yang et al., 2015; Quester et al., 2016; Cascio et al., 2014; Franci et al., 2015). However, the *in vivo* applications of AgNPs in crop protection have rarely been examined (Mishra et al., 2017).

To date, various chemical and physical approaches have been used for synthesizing and stabilizing AgNPs (Darroudi et al., 2011; Hussain et al., 2011; Khodashenas and Ghorbani, 2015). Recently, cost-effective and environmentally benign biosynthesis-based methods like "green synthesis" have been developed worldwide for production of NPs, including AgNPs (Rahi and Barwal, 2015; Lee et al., 2016; Cerda et al., 2017). These biological methods are more advantageous over the traditional toxic-chemical methods in terms of safety, efficiency and biocompatibility (Xie et al., 2007; Kumar et al., 2014; Quester et al., 2016). Eukaryotic organisms such as fungi are considered outstanding candidates for "green synthesis" of AgNPs because of the large amount of the secreted enzymes that catalyze the reducing and capping reactions of AgNPs (Rahi and Barwal, 2015; Quester et al., 2016). However, for a biological process to effectively contest with chemical and physical syntheses, the efficient control of shape and average particle size is needed (Gericke and Pinches, 2006). It has been reported that the shape and size of AgNPs, as well as the physiological solubility and bioactivity mostly depend on the reaction conditions and growth kinetics of the applied microorganisms (Sanghi and Verma, 2010; Li et al., 2011; Quester et al., 2016). Therefore, it is crucial to perform experiments with variable sets of parameters, including pH, temperature, bioagents, substrate concentrations and reaction time. Several fungal species like *Aspergillus niger*, *Fusarium oxysporum*, *Neurospora crassa* and *Penicillium* spp. have been reportedly used for the biosynthesis of AgNPs; however, the antimicrobial activity of the synthesized AgNPs, especially in crop protection against pathogens, remains to be determined (Selvi and Sivakumar, 2012; Gade et al., 2013; Quester et al., 2016). Basidiomycetes is one of the most economically important classes of higher fungi due to their widespread utilization in traditional Asian-medicines. The use of basidiomycetes for ethnomedicine has been attributed to their antimicrobial and antioxidant properties (Cilerdžić et al., 2014; Rajesh and Dhanasekaran, 2014). Although several antimicrobial bioactive compounds have been identified from basidiomycetes (Sudisha and Shekar Shetty, 2009; Jogaiah et al., 2016), little attention has been given to their role in AgNP biological synthesis (Rahi and Barwal, 2015). Therefore, it is of great importance to discover new fungal strains for synthesizing AgNPs based on their biodiversity and biological activities, as well as examine the potential of AgNP applications in plant disease management.

In this study, we explored the application of basidiomycete extracts as a naturally available platform for the "green synthesis" of AgNPs. Initially, the basidiomycete species were selected based on their antimicrobial activities using an established gradient solvent extraction system. Out of the seven species examined, the methanol extract of *G. applanatum* exhibited the highest antimicrobial activities, and thus *G. applanatum* was further selected as a potential fungal candidate for biological synthesis of AgNPs. The formation and characterization of synthesized AgNPs were subsequently studied by UV–Vis absorption spectroscopy, fourier transform infrared (FTIR), X-ray diffraction (XRD), scanning electron microscopy (SEM) and transmission electron microscopy (TEM) techniques. Additionally, the synthesized AgNPs were evaluated for their antioxidant capacity, and for their *in vitro* and *in vivo* functions in inhibiting both clinical pathogens and phytopathogens, providing their potential in medical applications and in plant protection against various diseases.

## 2. Materials and methods

### 2.1. Chemicals

$AgNO_3$ was purchased from Sigma-Aldrich (St Louis, MO, USA). L-Ascorbic acid, 1,1-diphenyl-2-picrylhydrazyl

(DPPH), *n*-hexane, chloroform and methanol were procured from Merck (Darmstadt, Germany). Phenolic standards, including, protocatechuic acid, catechin, chlorogenic, epicatechin, ferulic acid and apigenin were obtained from Sigma-Aldrich. Millipore distilled water was used in all experiments.

### 2.2. Collection of basidiomycete species

A survey was conducted in the forest region of Sanakeri, Sirsi, Uttar Karnataka, India (14.6185°N 74.8354°E) from November to December 2015. The basidiomycetes free from diseases were collected and stored at 4 °C till further use. The basidiomycete species were identified by their double walled basidiospores, ornamented shape and other characteristics according to the procedure described in the literature. The identification of seven basidiomycete species, named from BT. MBKUD-1 to BT.MBKUD-7, was further confirmed by comparison to the specimen's collection at Department of Biotechnology and Microbiology, Karnatak University (Table S1) (Jogaiah et al., 2016).

### 2.3. Preparation of basidiomycete extracts

Basidiomycete samples, including *Polyphorus* sp. (BT. MBKUD-1), *Tyromyces duracinus* (BT.MBKUD-2), *Pleurotus florida* (BT.MBKUD-3), *G. lucidum* (BT.MBKUD-4), *G. applanatum* (BT.MBKUD-7), and two unidentified basidiomycetes (BT.MBKUD-5) and (BT.MBKUD-6), were washed thoroughly 2–3 times with running tap water followed by sterilized distilled water (SDW). The samples were then cut immediately into small pieces and air-dried on sterile blotting paper under shade. Dried samples were crushed using a sterile electric blender to obtain a fine-powdered form, and stored in sterile polyethylene bags before use. The dry powder from each species was extracted separately with the following gradient solvent system: *n*-hexane, chloroform, methanol and water by subjecting to the Soxhlet apparatus (Supelco-64826, Sigma-Aldrich). Each solvent extraction step was repeated thrice and filtered. The filtered extracts were concentrated separately using rotary flash evaporator (Buchii R-100 rotary evaporators, vacuum pump V-100). The crude extract with a final concentration of 500 μg $mL^{-1}$ (w/v) was further assessed for its antimicrobial activities against clinical pathogens and phytopathogens.

### 2.4. Antibacterial assay of basidiomycete extracts using nutrient agar plates

The antibacterial activities of the *n*-hexane, chloroform, methanol and water crude extracts of the seven basidiomycete species were assessed against five clinical bacterial pathogens (*Klebsiella pneumoniae*, *Escherichia coli*, *Staphylococcus aureus*, *Bacillus subtilis* and *Pseudomonas aeruginosa*) using agar disc diffusion method. The bacterial inoculum preparation was done by a direct colony suspension method recommended by National Committee for Clinical and Laboratory Standards (NCCLS). The bacterial inoculum suspension previously adjusted to $10^6$ CFU $mL^{-1}$ was uniformly spread on sterile nutrient agar (NA) plates using sterile glass swab. Sterile 6-mm diameter wells were prepared equidistantly around the margin of the inoculated NA plates using cork borer. 50 μL (500 μg $mL^{-1}$) of each crude extract was dispensed in the wells. A negative control was prepared using the respective solvent used to dissolve the test sample. The plates were incubated for 24 h at 35 ± 2 °C, and inhibition zone of the bacterial growth was measured in "mm". Each test was performed in triplicate.

### 2.5. Antifungal assay of basidiomycete extracts using potato dextrose agar plates

The antifungal activity of the *n*-hexane, chloroform, methanol and water extracts of the seven basidiomycetes was assessed against four phytopathogens (*Colletotrichum gloeosporioides*, *Colletotrichum capsici*, *Curvularia lunata* and *Botrytis cinerea*) using potato dextrose agar (PDA) plates. An aliquot of each crude extract was added to the PDA to obtain a final concentration of 500 μg $mL^{-1}$. Crude extract-containing PDA plates were inoculated with a 5-mm agar plug containing the respective pathogen fungus that had been grown on PDA (without extract) for 5 days. The plates were incubated at 25 ± 2 °C, and the radial growth of the *C. gloeosporioides*, *C. capsici*, *C. lunata* and *B. cinerea* phytopathogens was measured after one week. Each test was performed in triplicate.

### 2.6. Antimicrobial assays of G. applanatum fractions

All the *G. applanatum* fractions were subjected to antimicrobial assays at a final concentration of 200 μg $mL^{-1}$ against *C. capsici* and *S. aureus* as described above.

### 2.7. Column chromatography of G. applanatum methanol extract

The *G. applanatum* 70% methanol extract was dried in a rotary evaporator using a vacuum pump (v-700; BUCHI, Rotavapor R-3) at 50 °C. The dried methanol extract was partitioned between *n*-butanol and $H_2O$ (1:1, v/v). The *n*-butanol layer was filtered and concentrated, affording 12.09 g extract. An aliquot of the crude extract was chromatographed by C300 silica gel column chromatography (3 cm × 60 cm; AG Tokyo, Japan). The column was developed using a gradient solvent system starting with 100% chloroform and chloroform-methanol (8:2–5:5) as eluents to give six fractions.

### 2.8. Determination of bioactive compounds in G. applanatum fraction 3 using HPLC

Briefly, *G applanatum* fraction 3 was filtered and centrifuged at 15,000 rpm for 5 min. The supernatant was completely dried using a rotary evaporator, and the remnant was then dissolved in 1 mL MeOH. A volume of 60 μL of filtered fraction 3 was injected into HPLC (Shimadzu, Tokyo, Japan). The HPLC system includes a pump, a column oven, a diode array detector set to 280 nm, a data collection system (EZchrom Elite TM; Hitachi High-Technologies Corporation, Tokyo, Japan), a DGU-14A degasser and a SIL-10ADvp autosampler. Separation was conducted at 30 °C on Agilent® Eclipse XDB C-18 reversed-phase column (250 mm × 4.6 mm length, 5 μm particle size). Identification and quantitative analyses were conducted by comparison with authentic standards.

### 2.9. Biosynthesis of AgNPs

AgNPs were prepared by biological synthesis route using fraction 3 of the *G. applanatum* (BT.MBKUD-7) methanol extract as reducing and capping agent. A reaction mixture consisted of 10 mL of the *G. applanatum* fraction 3, 1 mL of 100 mM $AgNO_3$ and 89 mL SDW was subjected to various pHs (4, 5, 6, 7 and 8), temperatures (15, 20, 25, 30 and 35 °C) and incubation periods (2, 4, 6, 12 and 24 h). The color change in the incubated supernatant was observed as the indicator for the synthesis of AgNPs. The cell-free filtrate (without $AgNO_3$) was maintained as control under the same conditions.

### 2.10. Characterization of AgNPs

The presence of AgNPs was initially observed by the visual change in color. AgNP detection was further confirmed by UV–Vis spectrum of the tested sample recorded at 420 nm using spectra ranging from 300 to 600 nm at room temperature. The presence of possible interactions between protein and AgNPs, and their type of binding was analyzed using FTIR spectrum recorded in absorption mode with Perkin Elmer spectrometer (Spectrum 1000) along with KBr pellets. The crystal structure and composition of AgNPs were determined by a Shimadzu powder X-ray diffractometer (PXRD-7000) using Ag Kα radiation of $\lambda = 1.541$°A in the $2\theta$ range of 20–80°. The size of the AgNPs was calculated using the Debye-Scherrer's equation (Dubey et al., 2010).

$$\tau = k\lambda/(\beta \cos\theta) \quad (1)$$

where $\tau$ is the mean size of the crystalline NPs, $k$ is a dimensionless shape factor (0.9), $\lambda$ is the X-ray wavelength, and $\beta$ is the line broadening at full-width at half maximum (FWHM) of the XRD peak at the diffraction angle $\theta$. The surface morphology and the structural properties of AgNPs were characterized by SEM (SEM, Hitachi-7000) at 40 keV and TEM (JEOL JSM 100CX). The samples were fixed with 2.5% glutaraldehyde overnight at room temperature followed by dehydration with gradient alcohol (10–95%) for 20 min, and then in absolute alcohol for 2–5 min. The final specimen was coated with monolayer platinum for making the surface conducting. TEM micrographs of the sample were taken using the JEOL JSM 100CS instrument operated at an accelerating voltage of 200 kV and an AMT XR41-B 4-megapixel (2048 × 2048) CCD camera.

### 2.11. Assay for AgNP antioxidant activity

DPPH scavenging activity was measured using $IC_{50}$ values as previously described (Abdelrahman et al., 2014). DPPH solution was prepared in ethanol and added to a serial dilution of *G. applanatum*-synthesized AgNPs and *G. applanatum* fraction 3. The reaction mixture was kept for 30 min under dark conditions at room temperature. Thereafter, the absorbance was read at 520 nm. The effective concentration, having 50% radical inhibition activity ($IC_{50}$) expressed as μg $mL^{-1}$, was calculated from the graph of the free radical scavenging activity. L-Ascorbic acid was used as a positive control. All experiments were repeated in triplicate.

### 2.12. Assay for antibacterial activities of AgNPs

An aliquot of the aqueous AgNPs, $AgNO_3$, *G. applanatum* fraction 3 (at a final concentration of 50 μg $mL^{-1}$) and SDW was dispensed on sterilized filter paper disc. The discs were placed equidistantly around the margin of the NA plates containing *S. aureus* or *E. coli*, and then the plates were incubated for 24 h at 35 ± 2 °C. Zone of inhibition of the bacterial growth was measured in mm. Each test was performed in triplicate.

### 2.13. In vivo leaflet assay for AgNP antifungal activities

One-month-old tomato (*Solanum lycopersicum*) and strawberry (*Fragaria* × *ananassa*) leaves were treated with an aliquot of the aqueous AgNPs and *G. applanatum* fraction 3 at a final concentration of 0, 12.5, 25 and 50 μg $mL^{-1}$, respectively. Agar plugs (5 mm in diameter) containing phytopathogen *B. cinerea* or C. *gloeosporioides*, which were grown on PDA for 5 days, were placed on AgNPs-wetted tomato and strawberry leaves, respectively. The treated leaves were incubated in sterilized plastic box for 7 days at 25 ± 2 °C under dark conditions. The development of disease was evaluated and recorded on the basis of the diameter of the necrotic lesion.

### 2.14. Statistical analysis

Data represented as means ± standard errors (SEs) of three repeats. The statistical analysis was performed by analysis of variance (ANOVA) using SPSS 20.0 (SPSS, Inc. USA). Heatmap clustering and box plot analysis were performed using R statistical package version 3.2.2 (www.r-project.org).

## 3. Results and discussion

The capping and reducing agents, as well as the reaction conditions, are crucial factors for the efficient production of AgNPs. Fungal extracts provide a useful platform for improving the "green synthesis" of AgNPs; however, the great difference in the biochemical constituents of each fungal species may significantly affect the AgNP biosynthesis process (Sanghi and Verma, 2010; Li et al., 2011; Quester et al., 2016). Therefore, it is of great importance to explore new fungal species with unique biochemical properties for AgNP biosynthesis. In this study, we developed a new approach to maximize the "green synthesis" of AgNPs, including (i) hierarchical clustering of seven basidiomycetes collected from the forest region of Sanakeri forest belt, Karnataka, India on the basis of their antimicrobial activity against clinical pathogens and phytopathogens, (ii) in-depth biochemical characterizations of the selected fungal species using liquid chromatography and antimicrobial assays, (iii) HPLC analysis for providing further insight with regard to the quality and quantity of the bioactive molecules, (iv) in-depth characterizations of the synthesized AgNPs by using UV–Vis absorption spectroscopy, FTIR, XRD, SEM and TEM, (v) evaluation of the antioxidant capacity and *in vitro* antibacterial activities of the synthesized AgNPs against clinical pthogens and (vi) evaluation of *in vivo*

antifungal properties against *B. cinerea* and *C. gloeosporioides* in tomato and strawberry leaflet assays, respectively. The current approach indicates the significant role of the *G. applantum* phenolic content in the "green synthesis" of AgNPs and subsequent antimicrobial activity. The obtained results are discussed in detail in the following sections.

### *3.1. G. applanatum is the most effective antibacterial and antifungal basidiomycete for AgNP synthesis among the seven investigated basidiomycetes*

The present study deals with the "green synthesis" of AgNPs using *G. applanatum* extract as reducing and capping agent, followed by the morphological and structural characterizations of synthesized AgNPs, as well as evaluation of their antimicrobial and antioxidant properties. Recently, syntheses of NPs using different fungal species have been reported (Devi and Joshi, 2015; Govindappa et al., 2016; Quester et al., 2016). Eukaryotic microbes, such as fungi, are considered as an exceptional choice for synthesizing NPs because they produce a great amount of secreted enzymes and proteins responsible for the bio-reduction (Gade et al., 2013; Cilerdžić et al., 2014). In addition, stabilizing and capping properties of the agents produced by fungi offer important advantages in "green synthesis" of NPs, including AgNP (Gade et al., 2013; Tran et al., 2013; Quester et al., 2016).

Among the microorganisms, the basidiomycetes produce a wide range of biologically active metabolites that have scarcely been investigated. A broad spectrum of natural products with biological activity produced by basidiomycetes includes antimicrobial, antifungal and antiviral compounds (Anke, 1989), as well as plant growth regulators (Jogaiah et al., 2016). Although various investigations reported the useful bioactive compounds from basidiomycetes, not much atten-

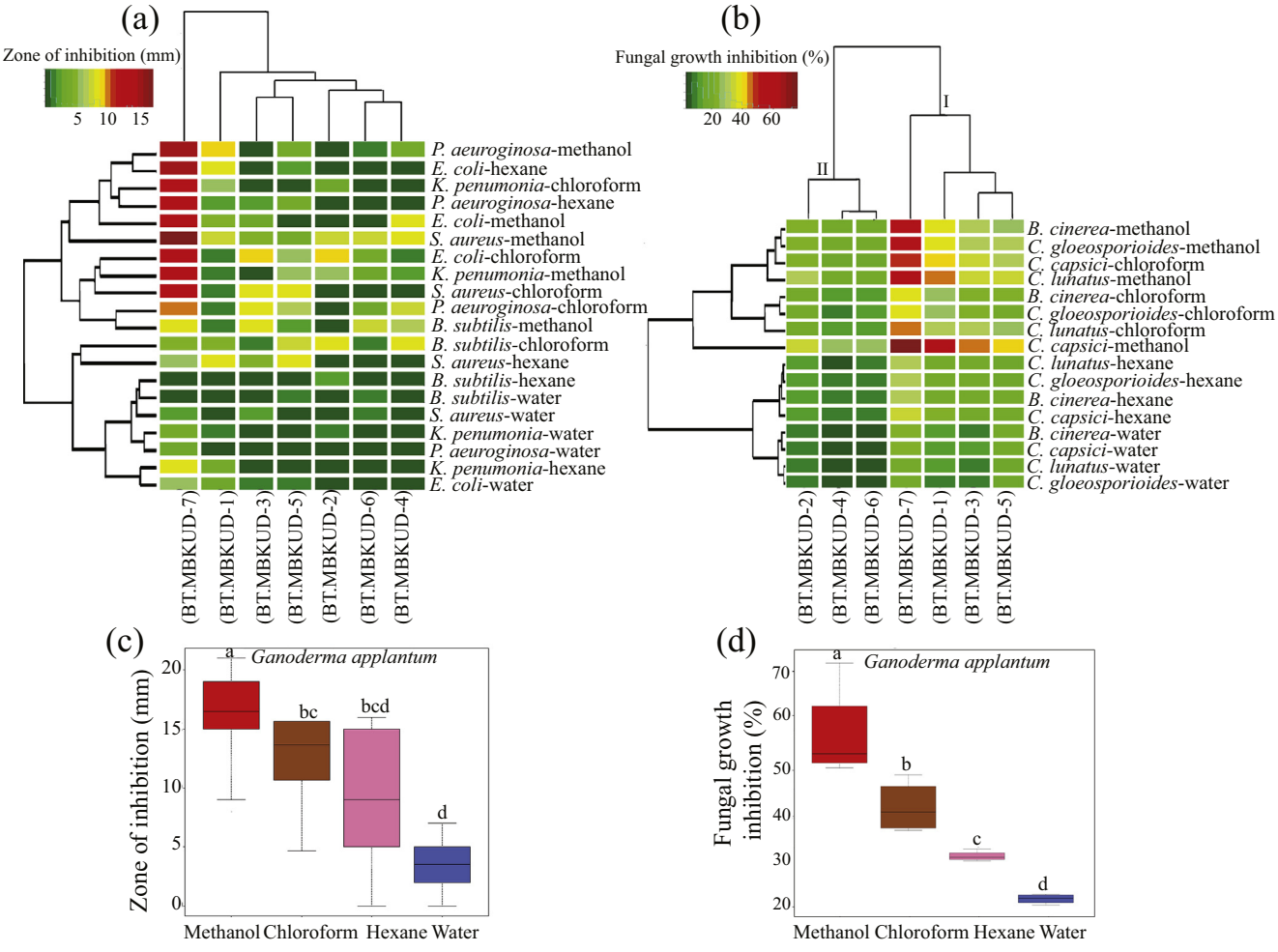


**Fig. 1** Antibacterial and antifungal properties of several basidiomycete extracts (500 μg $mL^{-1}$) using the gradient solvent system of *n*-hexane, chloroform, methanol and water. (a) Heatmap clustering of antibacterial activities of different solvent extracts from the *Polyphorus* sp. (BT.MBKUD-1), *Termitomyces microcarpus* (BT.MBKUD-2), *Pleurotus florida* (BT.MBKUD-3), *Ganoderma lucidum* (BT.MBKUD-4), *G. applanatum* (BT.MBKUD-7) and two unidentified basidiomycete species (BT.MBKUD-5 and BT.MBKUD-6). (b) Heatmap clustering of antifungal activities of different solvent extracts from seven basidiomycete species. (c) Box plot analysis of *G. applanatum* BT.MBKUD-7 antibacterial activities. (d) Box plot analysis of *G. applanatum* BT.MBKUD-7 antifungal activities. The heatmap color scale showed the antimicrobial range. Box plots labeled by the same letter(s) are not significantly different according to a Tukey's honestly significant difference *post hoc* test.

**Table 1** Determination of bioactive compounds in *Ganoderma applanatum* fraction 3 using high-performance liquid chromatography. Values are means ± standard errors (n = 3).

| Compounds | *Ganoderma applanatum* F3 (μg $g^{-1}$ extract) |
|---|---|
| Protocatechuic acid | 189 ± 2.10 |
| Catechin | 103 ± 3.24 |
| Chlorogenic acid | 33 ± 1.39 |
| Epicatechin | 17 ± 3.70 |
| Ferulic acid | 87 ± 3.25 |
| Apigenin | 120 ± 4.21 |

tion has been paid on the "green synthesis" of NPs using this microbial origin. Hence, in this study, we were interested in examining whether basidiomycetes could effectively synthesize AgNPs with antioxidant and antimicrobial activities, which can be then used in plant protection against various pathogens as well as in medical industry. In order to determine the most effective fungal basidiomycete species among the seven basidiomycetes examined, we first discriminated these basidiomycetes based on their antibacterial and antifungal activities using the gradient solvent extraction system of *n*-hexane, chloroform, methanol and water. The obtained results

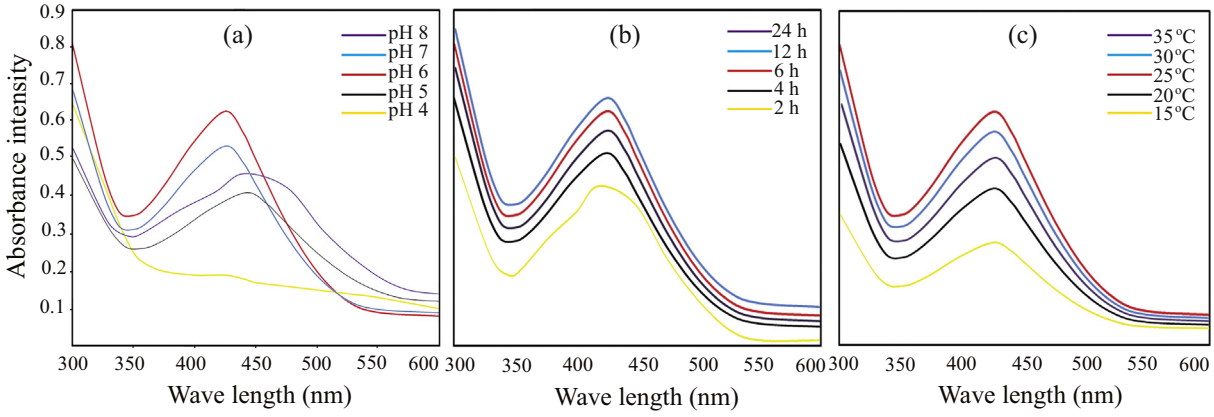


**Fig. 2** UV–Vis spectra of silver nanoparticles synthesized by *Ganoderma applanatum* fraction 3 at (a) different pHs, (b) incubation times (hours) and (c) temperatures.

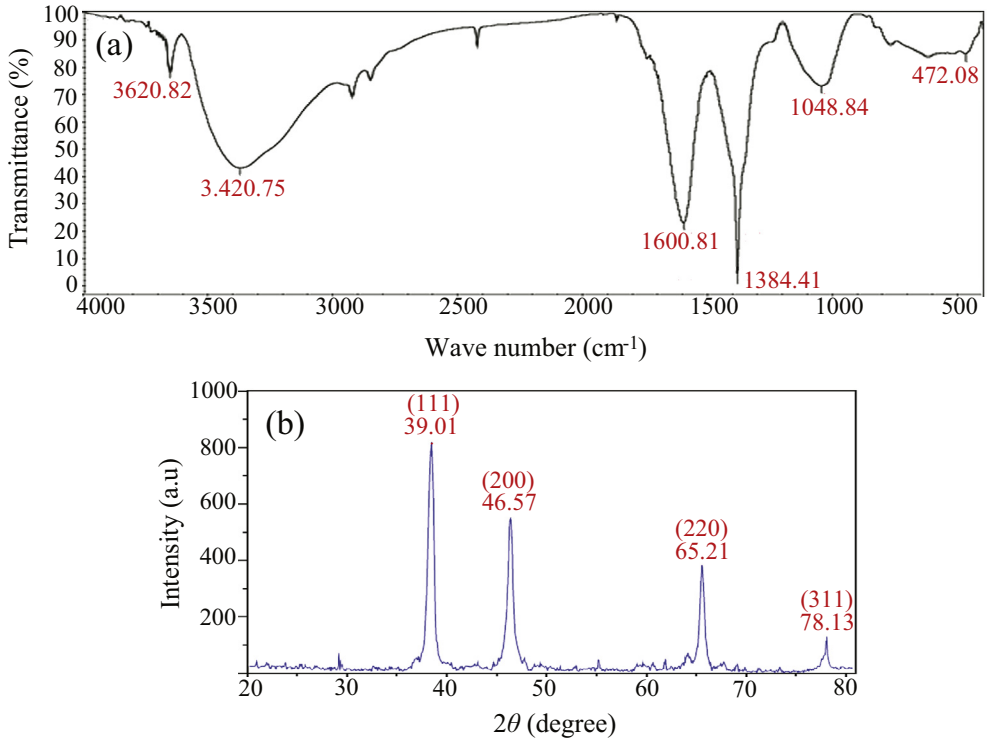


**Fig. 3** The core-shell morphology and crystalline pattern of *Ganoderma applanatum*-synthesized silver nanoparticles (AgNPs). (a) Fourier transform infrared spectroscopy and (b) X-ray diffraction of AgNPs synthesized by *G. applanatum* fraction 3. The infrared spectroscopy wave numbers and the Bragg reflections with 2$\theta$ values are shown within each corresponding peak.

were further subjected to heatmap clustering and box plot analysis (Fig. 1). The heatmap clustering results revealed a distinctive separation between the seven basidiomycete species, and *G. applanatum* extracts had the highest antibacterial and antifungal activities against the tested pathogens in comparison with that of other basidiomycetes (Fig. 1a, b). Additionally, box plot analysis of different *G. applanatum* solvent extracts indicated that the methanol extract exhibited the most significant antibacterial and antifungal activities against the tested pathogens as compared with other solvent extractions (Fig. 1c, d). *G. applanatum* methanol extract displayed the maximum bacterial growth inhibition with 18.50 mm inhibition zone against *S. aureus*, and the highest fungal growth inhibition of 75.49% against *C. capsici* (Fig. 1a and b). Therefore, *G. applanatum* methanol extract was further used for the "green synthesis" of AgNPs.

To optimize the efficacy and concentration of the *G. applanatum* methanol extract with regard to its antimicrobial properties, *G. applanatum* methanol extract was entirely freeze-dried and subjected to a column chromatography, resulting in 6 fractions. The obtained fractions were assessed for their antimicrobial activities at a final concentration of 200 μg $mL^{-1}$ (Fig. S1). Fraction 3 displayed a significantly higher antimicrobial activity in comparison with other tested fractions (Fig. S1), exhibiting 41.02% fungal growth inhibition against *C. capsici* and 10.13 mm inhibition zone against *S. aureus*. These data suggested that *G. applanatum* fraction 3 might contain the highest concentration of potential bioactive compounds that may induce the antimicrobial properties of AgNPs. To gain an insight into the nature of these key bioactive compounds in fraction 3, phytochemical analysis using HPLC-UV was carried out (Fig. S2 and Table 1). The HPLC results showed high phenolic contents in fraction 3, including protocatechuic acid, catechin and apigenin (Table 1). In support of our result, a recent finding reported that a *G. applanatum* strain has high phenolic contents, and these phenolic compounds are key components for the biological activities of *G. applanatum* (Zengin et al., 2015). The important role of phenolic compounds derived from plant extracts as potent antimicrobial and antioxidant agents has been well-

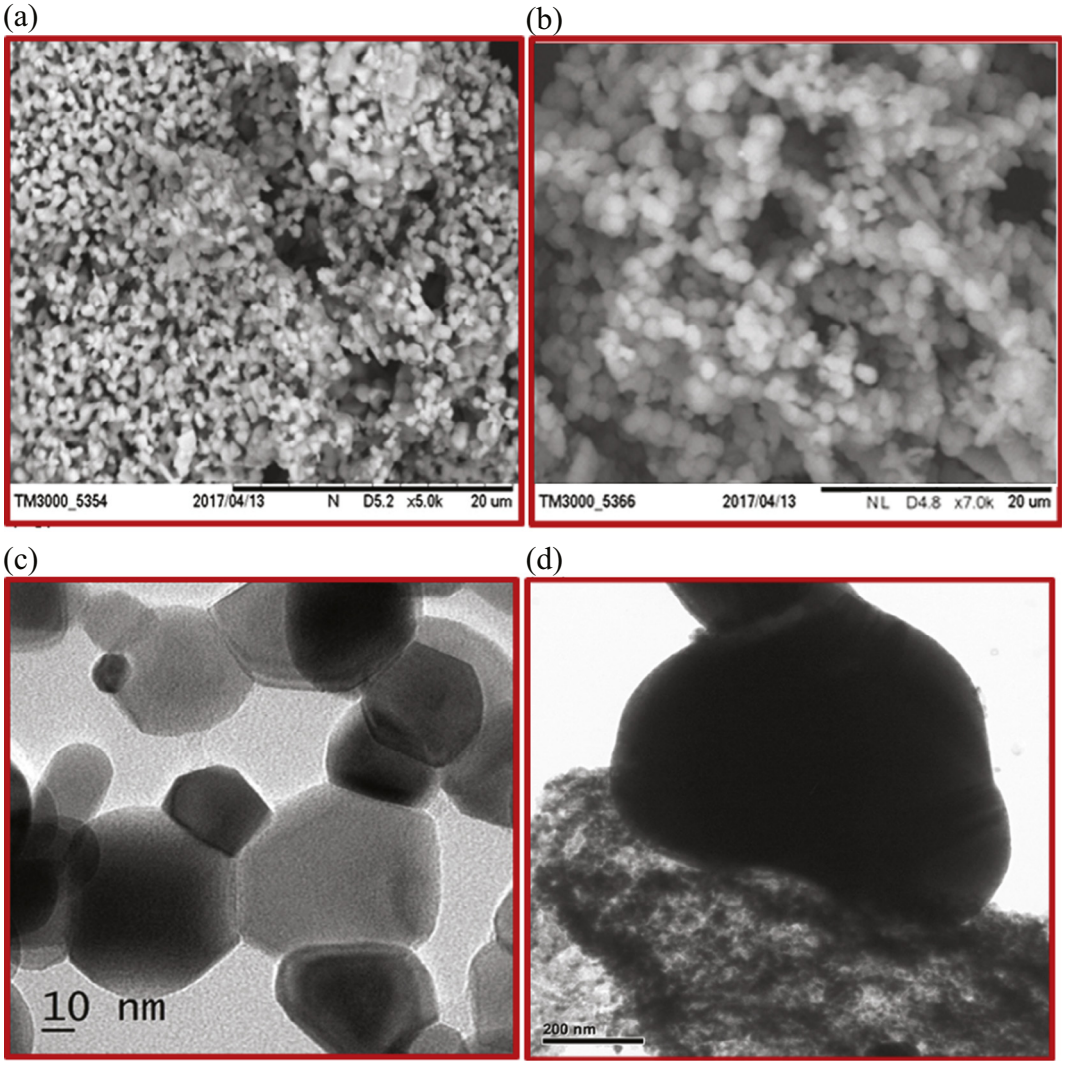


**Fig. 4** Scanning electron microscopic (SEM) and transmission electron microscopic (TEM) images of silver nanoparticles (AgNPs) synthesized by *Ganoderma applanatum*. (a) and (b) SEM images at different magnifications. (c) and (d) TEM micrographs showed the spherical AgNPs at different magnifications.

**Table 2** Antioxidant activities of *Ganoderma applanatum* aqueous fraction 3, *G. applanatum*-synthesized silver nanoparticles (AgNPs) and ascorbic acid (positive control). Values are means ± standard errors of three independent biological replicates. DPPH, 1,1-diphenyl-2-picrylhydrazyl.

| | DPPH $IC_{50}$ (μg $mL^{-1}$) |
|---|---|
| *G. applanatum* fraction 3 | 118.62 ± 5.89 |
| AgNPs | 98.73 ± 3.45 |
| Ascorbic acid | 37.53 ± 2.16 |

established, which was attributed to the presence of a hydroxyl group bonded to the aromatic hydrocarbon ring (Abdelrahman et al., 2015; Fatrcova-Sramková et al., 2016; Tohma et al., 2016).

The reaction mixture consisted of the *G. applanatum* fraction 3 and $AgNO_3$ was subjected to different conditions of pH, temperature and incubation period in order to optimize the uniformity and size of AgNPs. The reduction of $AgNO_3$ to AgNPs was visually detected by the change in color of the mixture from pale yellow to dark brown, which indicated the formation of AgNPs. UV–Vis absorbance spectra of the synthesized AgNPs at different pHs, temperatures and incubation time points were then recorded (Fig. 2). Strong and broad surface plasmon resonance (SPR) peak was observed at 420 nm at pH 6–7, which demonstrated the synthesis of AgNPs (Fig. 2). Previous studies suggested that an SPR peak between 410 and 450 nm is characteristic for AgNPs, and might be attributed to spherical NPs (Rafiuddin, 2012; Jyoti et al., 2015). The main absorption band for AgNPs was shifted to higher unresolved absorption wavelength for AgNPs formed at other pH values, indicating that the synthesized AgNPs at these pHs are not spherical, and may exhibit different sizes and shapes (Fig. 2a). Likewise, the time-course analysis of AgNP biosynthesis process by *G. applanatum* fraction 3 clearly demonstrated the rapid biosynthesis of AgNPs as evidenced by the

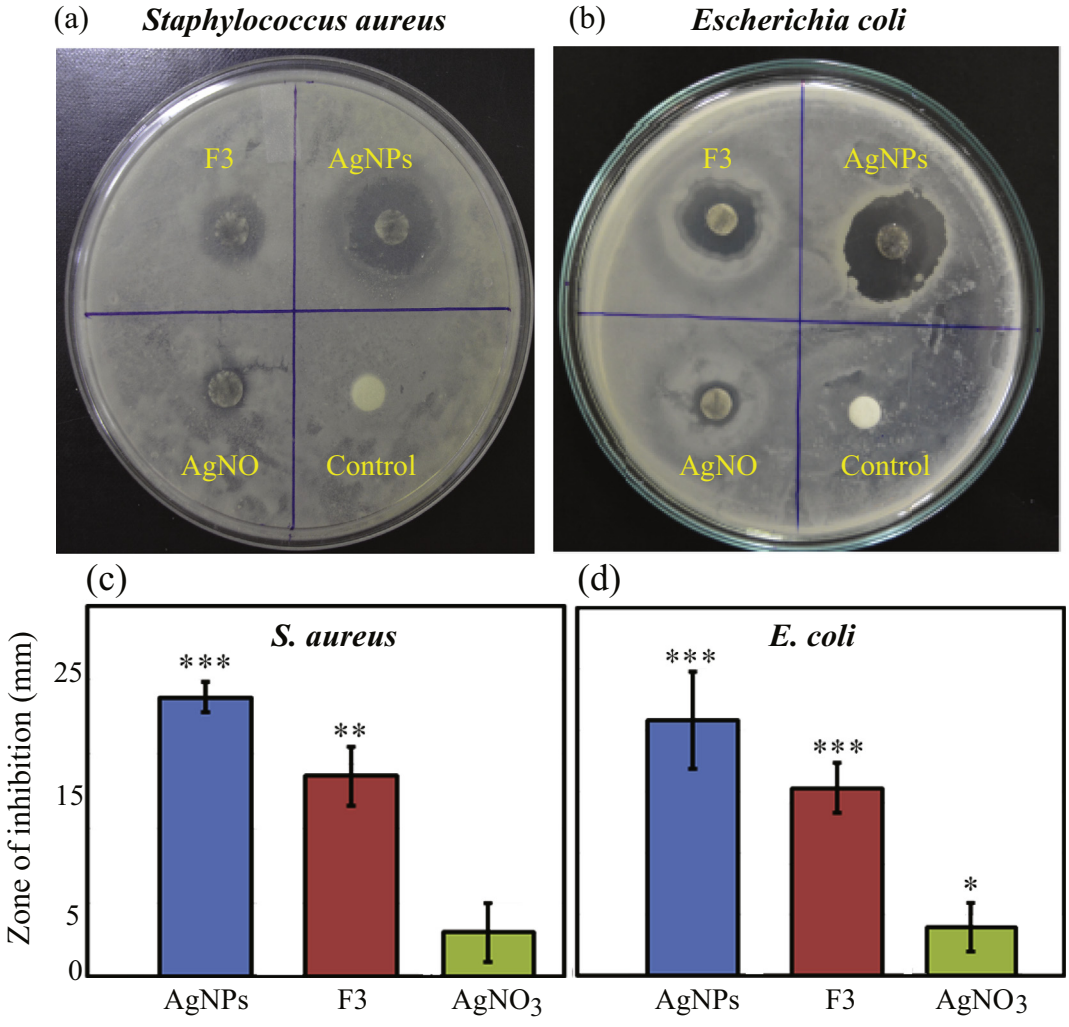


**Fig. 5** Antibacterial activities of silver nanoparticles (AgNPs) synthesized by *Ganoderma applanatum* fraction 3. (a) and (b) Images showing antibacterial activities of AgNPs at a final concentration of 50 μg $mL^{-1}$ against *Staphylococcus aureus* and *Escherichia coli*, respectively. (c) and (d) The diameter of inhibition zone in *S. aureus* and *E. coli*, respectively. Values are means ± standard errors (n = 3). Significance levels between control versus AgNPs, control versus *G. applanatum* fraction 3 (F3), and control versus $AgNO_3$ (50 μg $mL^{-1}$) are indicated by asterisks ($^{*}P < .05$, $^{**}P < .01$ and $^{***}P < .001$) according to an independent Student's *t*-test.

absorbance intensity at 2 h, and the increase in the incubation time accelerated the AgNP biosynthesis process with maximum absorbance intensity being detected at 6 and 12 h (Fig. 2b). The effect of temperature on the rate of AgNP biosynthesis by *G. applanatum* fraction 3 showed a characteristic absorbance of the synthesized AgNPs at 420 nm with maximum absorbance intensity being observed at 25 and 30 °C (Fig. 2c).

### *3.2. Characterization of the synthesized AgNPs by FTIR and X-ray diffraction*

FTIR is a valuable tool to investigate the core-shell morphology of the synthesized AgNPs, and also provides crucial information about the chemical bonds and molecular structures responsible for the bio-reduction of $Ag^{+}$ and capping/stabilization of the AgNPs (Jyoti et al., 2015). The observed bands

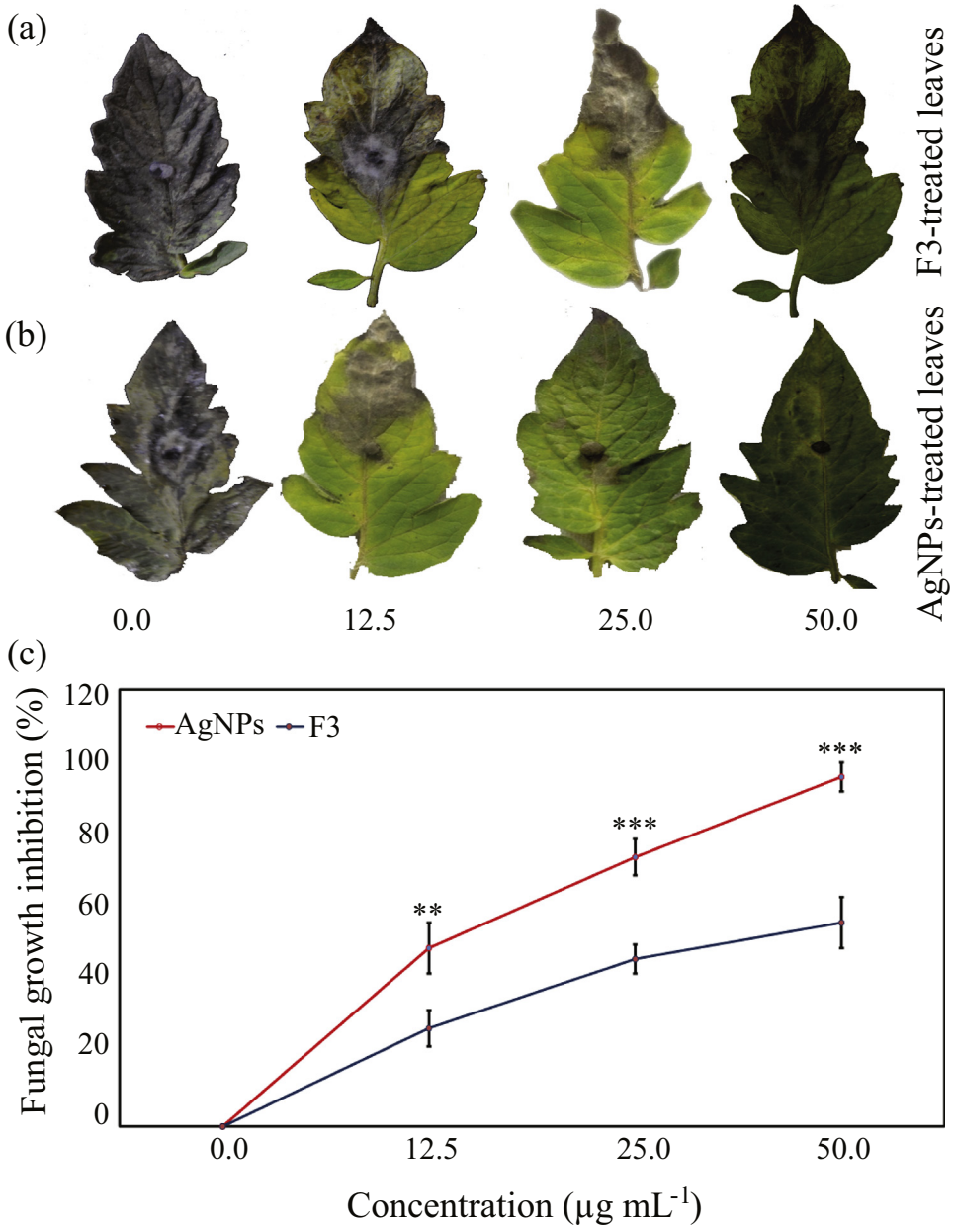


**Fig. 6** Antifungal activities of silver nanoparticles (AgNPs) synthesized by *Ganoderma applanatum* fraction 3 (F3). (a) and (b) *In vivo* antifungal leaflet assay of one-month-old tomato leaves treated with different concentrations of F3 or AgNPs (0, 12.5, 25 and 50 μg $mL^{-1}$), and then challenge-inoculated with *Botrytis cinerea*. (c) Fungal growth inhibition percentage of *B. cinerea*. Values are means ± standard errors (n = 3). Significance difference between F3 and AgNPs at each concentration is indicated by asterisks ($^{*}P < .05$, $^{**}P < .01$ and $^{***}P < .001$) according to an analysis of variance test.

were compared with standard values to identify the functional groups. FTIR spectra showed absorption bands at 3620.82, 3420.75, 1600.81, 1384.41, 1048.84 and 472.08 $cm^{-1}$ (Fig. 3a), indicating the presence of capping agent with the NPs. The bands from 3620.82 to 3420.75 $cm^{-1}$ correspond to O—H stretching, indicating the presence of alcohol and phenol. The band at 1600.81 $cm^{-1}$ in the spectra corresponds to N = O and C = O stretches, indicating the presence of amide and nitro groups. The bands from 1384.41 to 1048.84 $cm^{-1}$ correspond to the C—O and N = O stretches, indicating the presence of nitro and ester groups, respectively. These functional groups have an important role in the stability/capping and biological activities of AgNPs (Jyoti et al., 2015; Prakash et al., 2013). The FTIR data indicated that the synthesized AgNPs were enclosed by *G. applanatum* proteins and amino acids, which may be responsible for the stability of the AgNPs, and that the structure of proteins derived from *G. applanatum* was not affected by the interactions with synthesized AgNPs.

### *3.3. Characterization of synthesized AgNPs by XRD, SEM and TEM*

The crystalline pattern of AgNPs was further verified by X-ray crystallography, and the XRD of the synthesized AgNPs was recorded (Fig. 3b). The diffracted intensities were recorded

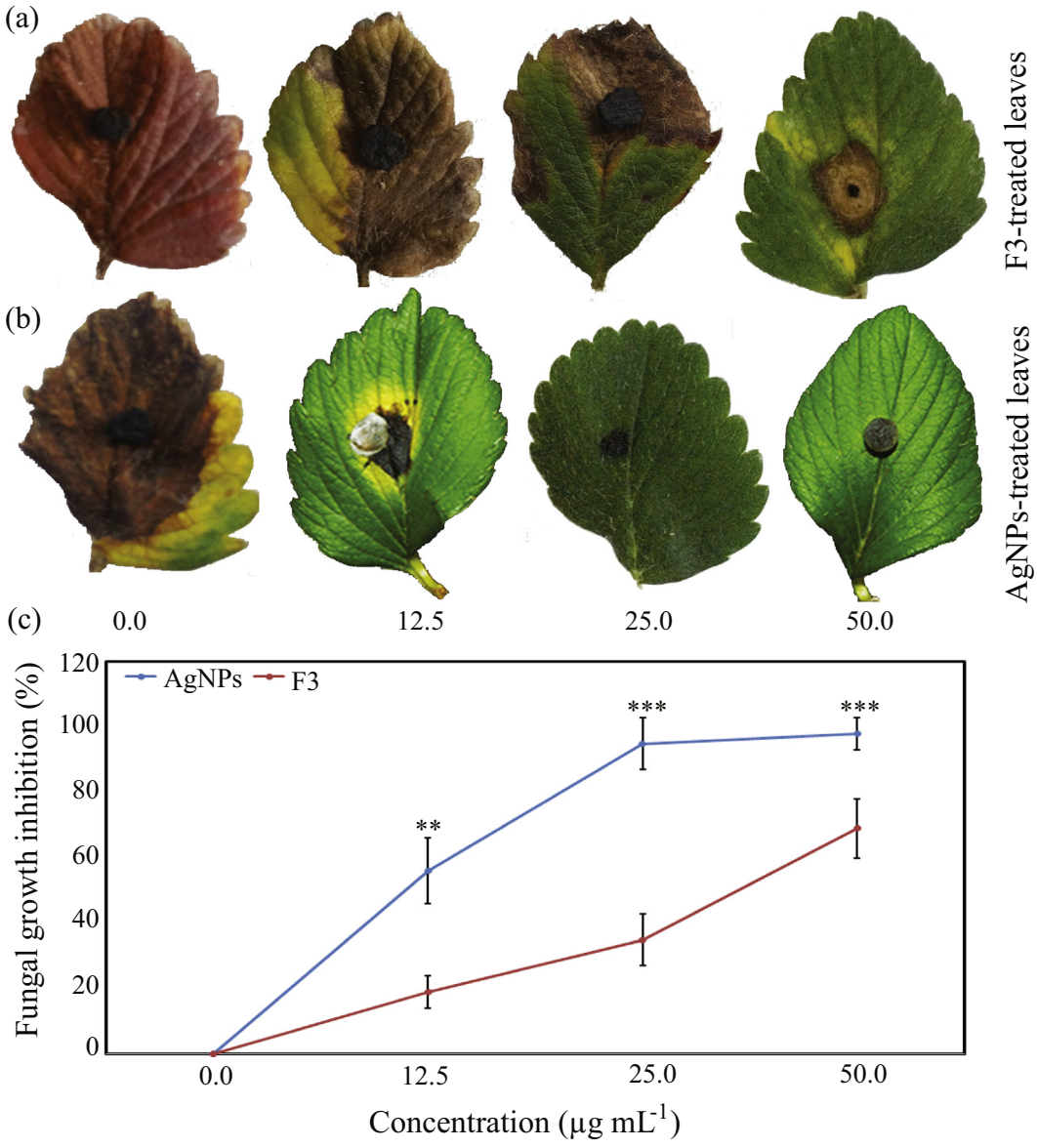


**Fig. 7** Antifungal activities of silver nanoparticles (AgNPs) synthesized by *Ganoderma applanatum* fraction 3 (F3). (a) and (b) *In vivo* antifungal leaflet assay of one-month-old strawberry leaves treated with different concentrations of F3 or AgNPs (0, 12.5, 25 and 50 μg $mL^{-1}$), and then challenge-inoculated with *Colletotrichum gloeosporioides*. (c) Fungal growth inhibition percentage of *C. gloeosporioides*. Values are means ± standard errors (n = 3). Significance difference between F3 and AgNPs at each concentration is indicated by asterisks ($^{*}P < .05$, $^{**}P < .01$ and $^{***}P < .001$) according to an analysis of variance test.

from 20° to 80°. The Bragg reflections with 2$\theta$ values of 39.01°, 46.57°, 65.21° and 78.13° corresponded to the (1 1 1), (2 0 0), (2 2 0) and (3 1 1) sets of lattice planes indicated the bands for face-centered cubic structure of Ag and its crystalline nature (Prakash et al., 2013). The calculated crystallite size of the AgNPs ranged from 20 to 25 nm.

SEM and TEM studies provide further insight into the morphology and particle size distribution profile of the AgNPs (Fig. 4). The SEM micrograph recorded at different magnifications indicated the AgNP aggregates (Fig. 4a, b). The SEM micrograph showed the spherical AgNPs in the size ranged between 20 and 25 nm Additionally, TEM images provided further details of the morphology of the synthesized AgNPs (Fig. 4c, d). The spherical nature of the AgNPs was also verified by TEM analysis with an average diameter between 20 and 25 nm. Thus, both SEM and TEM results strengthened the XRD crystalline size of the synthesized AgNPs.

### 3.4. Antioxidant activity of the synthesized AgNPs

The antioxidant activity of the *G. applanatum*-synthesized AgNPs and *G. applanatum* fraction 3 was evaluated using the DPPH $IC_{50}$ scavenging assay, with ascorbic acid being a positive standard. The maximum DPPH scavenging activity was recorded with ascorbic acid ($IC_{50}$, 37.53 μg $mL^{-1}$) and AgNPs ($IC_{50}$, 98.73 μg $mL^{-1}$), whereas the lowest scavenging activity was recorded for the *G. applanatum* fraction 3 ($IC_{50}$, 118.62 μg $mL^{-1}$) (Table 2). Our data were in line with the results of previous studies that have reported the antioxidant activities of AgNPs synthesized using the crude extracts derived from *Chenopodium murale*, *Bergenia ciliate* and *Malus domestica* (Abdel-Aziz et al., 2014; Nagaich et al., 2016; Phull et al., 2016). It is well-established that the antioxidant activity is majorly attributed to the phenolic contents of the living organism (Abdelrahman et al., 2016). The FTIR data demonstrated the presence of phenol groups (Fig. 3a) in *G. applanatum*-synthesized AgNPs which may contribute to their DPPH scavenging activity.

### 3.5. In vitro antibacterial activities of the synthesized AgNPs

Next, the antibacterial activities of *G. applanatum*-synthesized AgNPs were evaluated against two clinical bacterial pathogens (*S. aureus* and *E. coli*) using agar disc diffusion method (Fig. 5a, b). At the final concentration of 50 μg $mL^{-1}$, the AgNPs exhibited higher antibacterial activities against *S. aureus* (16.33 mm) and *E. coli* (13.33 mm) in comparison with the crude *G. applanatum* fraction 3 (7.4 and 6.8 mm, respectively) and $AgNO_3$ (1.83 and 0.85 mm, respectively) (Fig. 5c, d). The differential antibacterial activities between AgNPs and $AgNO_3$ clearly demonstrate the importance of *G. applanatum* extract in the improvement of the antibacterial properties of the synthesized AgNPs. In support of our findings, antibacterial activities of AgNPs, which were synthesized from *Mimusops elengi* leaf extract and the marine bacterium *Ochrobactrum anhtropi*, against various clinical pathogens were also reported (Zhou et al., 2012; Prakash et al., 2013; Thomas et al., 2014; Le Ouay and Stellacci, 2015). The antibacterial effect of AgNPs could be explained on the basis of small-sized AgNPs synthesized by *G. applanatum* and functional capping groups that provide a better interaction with the bacterial cell membranes (Zhou et al., 2012; Thomas et al., 2014; Le Ouay and Stellacci, 2015). In addition, AgNP interaction with bacterial cell membrane will facilitate the $Ag^+$ penetration and interactions with cellular DNA and proteins, resulting in loss of cell viability and cell death (Rafiuddin, 2012; Le Ouay and Stellacci, 2015).

### 3.6. In vivo antifungal activities of the synthesized AgNPs

In the next line of our study, we were curious whether the synthesized AgNPs could provide protection to plants against phytopathogens. Leaflet assay was carried out using one-month-old tomato and strawberry leaves treated with different concentrations of AgNPs and *G. applantum* fraction 3 extract (0, 12.5, 25 and 50 μg $mL^{-1}$). The treated-tomato and -strawberry leaves were further inoculated with 5-mm PDA plug of *B. cinerea* and *C. gloeosporioides*, respectively (Figs. 6 and 7). The antifungal activities of synthesized AgNPs were significantly increased with the increasing concentrations of AgNPs (Figs. 6c and 7c). The maximum fungal growth inhibi-

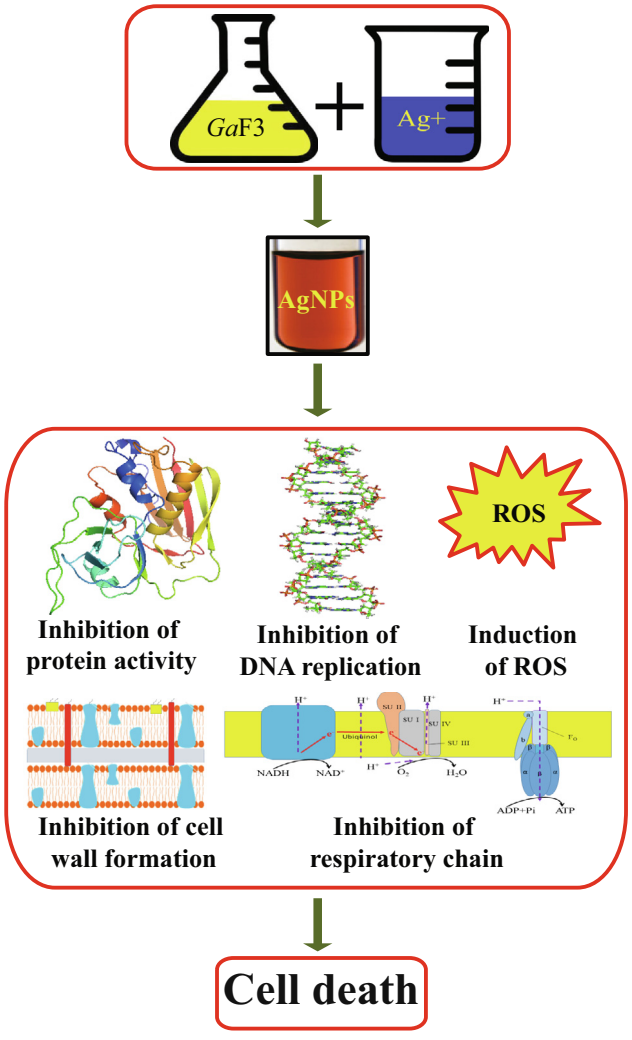


**Fig. 8** Potential antibacterial mechanisms of silver nanoparticles synthesized by *Ganoderma applanatum* fraction 3 (*Ga*F3). ROS, reactive oxygen species; $F_O$, a component of ATP synthase; α and β, membrane subunits of ATP synthase; SU I-IV, subunits of the cytochrome $bo_3$ ubiquinol oxidase.

tion was observed at 50 μg $mL^{-1}$ AgNPs, whereas tomato and strawberry leaves exhibited a full necrotic lesion and subsequent leaf wilting without AgNP treatment. The observed results showed the capability of AgNPs to prevent the fungal spreading in the inoculated-tomato and -strawberry leaves without affecting the leaf morphological status. In support of our findings, *in vitro* antifungal activities of AgNPs synthesized from turnip leaf extract and sodium citrate solution, against wood-degrading fungal pathogens (e.g. *Gloeophyllum abietinum*, *G. trabeum*, *Chaetomium globosum* and *Phanerochaete sordida*) and cotton pathogen *Rhizoctonia solani*, respectively, were reported in previous studies (Narayanan and Park, 2015; Elgorban et al., 2016; Haghighi Pak et al., 2016). However, the *in vivo* antifungal activity of AgNPs has rarely been examined. Thus, the finding of our *in vivo* antifungal assay provides strong support for the development of agrochemical NP agents with the cost-effective and environmentally acceptable platform. Further studies are required to determine the efficacy of AgNPs against various phytopathogens in different cropping systems under controls and field conditions for their broad and efficient applications in agriculture. The hypothetical antimicrobial mechanism of AgNPs has been summarized in Fig. 8. Taken together, it can be concluded that the "green synthesis" of AgNPs using *G. applanatum* extract is a cost-effective and environmentally acceptable platform that excludes the hazards resulted from the use of toxic reducing/capping agents. Moreover, this process could be simply scaled up for the industrial applications to maximize the yield of the AgNPs.

## Notes

The authors declare no conflict of interest.

## Acknowledgements

SJ sincerely thanks the Department of Biotechnology and Microbiology, Karnatak University, for laboratory and field facilities.

## Appendix A. Supplementary material

Supplementary data associated with this article can be found, in the online version, at https://doi.org/10.1016/j.arabjc.2017.12.002.

## References

Abdel-Aziz, M.S., Shaheen, M.S., El-Nekeety, A.A., Abdel-Wahha, M.A., 2014. Antioxidant and antibacterial activity of silver nanoparticles biosynthesized using *Chenopodium murale* leaf extract. J. Saudi Chem. Soc. 18, 356–363.

Abdelrahman, M., Abdel-Motaal, F., El-Sayed, M., Jogaiah, S., Shigyo, M., Ito, S.-I., Tran, L.S., 2016. Dissection of *Trichoderma longibrachiatum*-induced defense in onion (*Allium cepa* L.) against *Fusarium oxysporum* f. sp. *cepa* by target metabolite profiling. Plant Sci. 246, 128–138.

Abdelrahman, M., Hirata, S., Ito, S., Yamauchi, N., Shigyo, M., 2014. Compartmentation and localization of bioactive metabolites in different organs of *Allium roylei*. Biosci. Biotechnol. Biochem. 78, 1112–1122.

Abdelrahman, M., Sawada, Y., Nakabayashi, R., Sato, S., Hirakawa, H., El-Sayed, M., Hirai, M.Y., Saito, K., Yamauchi, N., Shigyo, M., 2015. Integrating transcriptome and target metabolome variability in doubled haploids of *Allium cepa* for abiotic stress protection. Mol. Breed. 35, 195.

Anke, T., 1989. Basidiomycetes: a source for new bioactive secondary metabolites. Prog. Ind. Microbiol. 27, 51–66.

Cascio, C., Gilliland, D., Rossi, F., Calzolai, L., Contado, C., 2014. Critical experimental evaluation of key methods to detect, size and quantify nanoparticulate silver. Analy. Chem. 86, 12143–12151.

Cerda, S.J., Gomez, E.H., Nunez, A.G., Rivero, I.A., Ponce, G.Y., Lopez, F.L.Z., 2017. A green synthesis of copper nanoparticles using native cyclodextrins as stabilizing agents. J. Saudi Chem. Soc. 21, 341–348.

Chaudhuri, G.R., Paria, S., 2012. Core/Shell nanoparticles: classes, properties, synthesis mechanisms, characterization, and applications. Chem. Rev. 112, 2373–2433.

Cilerdžić, J., Vukojević, J., Stajić, M., Stanojković, T., Glamočlija, J., 2014. Biological activity of *Ganoderma lucidum* basidiocarps cultivated on alternative and commercial substrate. J. Ethnopharmacol. 155, 312–319.

Darroudi, M., Ahmad, M.B., Abdullah, A.H., Ibrahim, N.A., 2011. Green synthesis and characterization of gelatin-based and sugar-reduced silver nanoparticles. Int. J. Nanomed. 6, 569–574.

Devi, L.S., Joshi, S.R., 2015. Ultrastructures of silver nanoparticles biosynthesized using endophytic fungi. J. Microsc. Ultrastruct. 3, 29–37.

Dubey, S.P., Lahtinen, M., Sillanpaa, M., 2010. Tansy fruit mediated greener synthesis of silver and gold nanoparticles. Process Biochem. 45, 1065–1071.

Elgorban, A.M., El-Samawaty, A.M., Yassin, M.A., Sayed, S.R., Adil, S.F., Elhindi, K.M., Bakri, M., Khan, M., 2016. Antifungal silver nanoparticles: synthesis, characterization and biological evaluation. Agric. Environ. Biotechnol. 30, 56–62.

Fatrcova-Sramková, K., Nozková, J., Mariassyová, M., Kacaniová, M., 2016. Biologically active antimicrobial and antioxidant substances in the *Helianthus annuus* L. bee pollen. J. Environ. Sci. Health 51, 176–181.

Franci, G., Falanga, A., Galdiero, S., Palomba, L., Rai, M., Morelli, G., Galdiero, M., 2015. Silver nanoparticles as potential antibacterial agents. Molecules 20, 8856–8874.

Gade, A., Gaikwad, S., Duran, N., Rai, M., 2013. Screening of different species of *Phoma* for synthesis of silver nanoparticles. Biotechnol. Appl. Biochem. 60, 482–493.

Gericke, M., Pinches, A., 2006. Biological synthesis of metal nanoparticles. Hydrometallurgy 83, 132–140.

Govindappa, M., Farheen, H., Chandrappa, C.P., Channabasava, Rai, R.V., Vinay, B.R., 2016. Mycosynthesis of silver nanoparticles using extract of endophytic fungi, *Penicillium* species of *Glycosmis mauritiana*, and its antioxidant, antimicrobial, anti-inflammatory and tyrokinase inhibitory activity. Adv. Nat. Sci. Nanosci. Nanotechnol. 7, 035014.

Haghighi Pak, Z., Abbaspour, H., Karimi, N., Fattahi, A., 2016. Eco-friendly synthesis and antimicrobial activity of silver nanoparticles using *Dracocephalum moldavica* seed extract. Appl. Sci. 6, 69.

Hussain, J.I., Kumar, S., Hashmi, A.A., Khan, Z., 2011. Silver nanoparticles: preparation, characterization, and kinetics. Adv. Mat. Lett. 2, 188–194.

Jogaiah, S., Shetty, H.S., Ito, S.-I., Tran, L.S., 2016. Enhancement of downy mildew disease resistance in pearl millet by the G_app7 bioactive compound produced by *Ganoderma applanatum*. Plant Physiol. Biochem. 105, 109–117.

Jyoti, K., Baunthiyal, M., Singh, A., 2015. Characterization of silver nanoparticles synthesized using *Urtica dioica* Linn. leaves and their synergistic effects with antibiotics. J. Rad. Res. Appl. Sci. 9, 217–227.

Kavyashree, D., AnandaKumari, R., Nagabhushana, H., Sharma, S. C., Vidya, Y.S., Anantharaju, K.S., Daruka Prasad, B., Prashantha, S.C., Lingaraju, K., Rajanaik, H., 2015. Orange red emitting Eu3+ doped zinc oxide nanophosphor material prepared using *Guizotia abyssinica* seed extract: structural and pho-toluminescence studies. J. Lumin. 167, 91–100.

Khodashenas, B., Ghorbani, H.R., 2015. Synthesis of silver nanoparticles with different shapes. Arab. J. Chem. https://doi.org/10.1016/j.arabjc.2014.12.014.

Kumar, N., Palmer, G.R., Shah, V., Walker, V.K., 2014. The effect of silver nanoparticles on seasonal change in arctic tundra bacterial and fungal assemblages. PLoS ONE 9, e99953.

Lakshmeesha, T.R., Sateesh, M.K., Daruka, P.B., Sharma, S.C., Kavyashree, D., Chandrashekar, M., Nagabhushana, H., 2014. Reactivity of crystalline ZnO superstructures against fungi and bacterial pathogens: Synthesized using *Nerium oleander* leaf extract. Cryst. Growth Des. 14, 4068–4079.

Le Ouay, B., Stellacci, F., 2015. Antibacterial activity of silver nanoparticles: a surface science insight. Nanotoday 10, 339–354.

Lee, K.X., Shameli, K., Miyake, M., Kuwano, N., Khairudin, N.B.B. A., Mohamad, S.E.B., Yew, Y.P., 2016. Green synthesis of gold nanoparticles using aqueous extract of *Garcinia mangostana* fruit peels. J. Nanomater. 2016, 7. Article ID 8489094.

Li, X., Xu, H., Chen, Z., Chen, G., 2011. Biosynthesis of nanoparticles by microorganisms and their applications. J. Nanomater. 2011, 16. Article ID 270974.

Mallmann, E.J.J., Cunha, F.A., Castro, B.N.M.F., Maciel, A.M., Menezes, E.A., Fechine, P.B.A., 2015. Antifungal activity of silver nanoparticles obtained by green synthesis. Rev. Inst. Med. Trop. Sao Paulo 57, 165–167.

Mishra, S., Singh, B.R., Naqvi, A.H., Singha, H.B., 2017. Potential of biosynthesized silver nanoparticles using *Stenotrophomonas* sp. BHU-S7 (MTCC 5978) for management of soil-borne and foliar phytopathogens. Sci. Rep. 7. https://doi.org/10.1038/srep45154.

Nagaich, U., Gulati, N., Chauhan, S., 2016. Antioxidant and antibacterial potential of silver nanoparticles: biogenic synthesis utilizing apple extract. J. Pharm. (Cairo). https://doi.org/10.1155/2016/7141523.

Narayanan, K.P., Park, H.H., 2015. Antifungal activity of silver nanoparticles synthesized using turnip leaf extract (*Brassica rapa* L.) against wood rotting pathogens. Eur. J. Plant Pathol. 140, 185–192.

Phull, A.-R., Abbas, Q., Ali, A., Raza, H., Kim, S.J., Zia, M., Haq, I.-U., 2016. Antioxidant, cytotoxic and antimicrobial activities of green synthesized silver nanoparticles from crude extract of *Bergenia ciliate*. Future J. Pharm. Sci. 2, 31–36.

Prakash, P., Gnanaprakasam, P., Emmanuel, R., Arokiyaraj, S., Saravanan, M., 2013. Green synthesis of silver nanoparticles from leaf extract of *Mimusops elengi*, Linn. for enhanced antibacterial activity against multi drug resistant clinical isolates. Colloids Surf. B: Biointerf. 108, 255–259.

Quester, K., Avalos-Borja, M., Castro-Longori, E., 2016. Controllable biosynthesis of small silver nanoparticles using fungal extract. J. Biomat. Nanobiotechnol. 7, 118–125.

Rafiuddin, Z.Z., 2012. Silver nanoparticles to self-assembled films: green synthesis and characterization. Colloids Surf. B: Biointerf. 90, 48–52.

Rahi, D.K., Barwal, M., 2015. Biosynthesis of silver nanopartciles by *Ganoderma applanatum*, evaluation of their antibacterial and antibiotic activity enhancing potential. World J. Pharma. Pharm. Sci. 4, 1234–1247.

Rajesh, K., Dhanasekaran, D., 2014. Phytochemical screening and biological activity of medicinal mushroom *Ganoderma* species. Malaya J. Biosci. 1, 67–75.

Rauwel, P., Rauwel, E., Ferdov, S., Singh, M.P., 2015. Silver nanoparticles: synthesis, properties, and applications. Adv. Mater. Sci. Eng. 2015, 624394.

Salem, W., Leitner, D.R., Zingl, F.G., Schratter, G., Prassl, R., Goessler, W., Reidl, J., Schild, S., 2015. Antibacterial activity of silver and zinc nanoparticles against *Vibrio cholerae* and enterotoxic *Escherichia coli*. Int. J. Med. Microbiol. 305, 85–95.

Sanghi, R., Verma, P., 2010. pH Dependent fungal proteins in the "green synthesis" of gold nanoparticles. Adv. Mater. Lett. 1, 193–199.

Selvi, K.V., Sivakumar, T., 2012. Isolation and characterization of silver nanoparticles from *Fusarium oxysporum*. Int. J. Curr. Microbiol. App. Sci. 1, 56–62.

Sudisha, J., Shekar Shetty, H., 2009. Anti-oomycete compounds from *Ganoderma applanatum*, a wood rot basidiomycete. Nat. Prod. Res. 23 (1), 737–753.

Thomas, R., Janardhanan, A., Varghese, R.T., Soniya, E.V., Mathew, J., Radhakrishnan, E.K., 2014. Antibacterial properties of silver nanoparticles synthesized by marine *Ochrobactrum* sp. Braz. J. Microbiol. 45, 1221–1227.

Tohma, H., Koksal, E., Kiliç, O., Alan, Y., Yılmaz, M.A., Gulçin, I., Bursal, E., Alwasel, S.H., 2016. RP-HPLC/MS/MS Analysis of the phenolic compounds, antioxidant and antimicrobial activities of *Salvia* L. Species. Antioxidants 5, 38.

Tran, Q.H., Nguyen, V.Q., Le, A.T., 2013. Silver nanoparticles: synthesis, properties, toxicology, applications and perspectives. Adv. Nat. Sci. Nanosci. Nanotechnol. 4, 033001.

Xie, J., Lee, J.Y., Daniel, I.C., Ting, Y.P., 2007. High-yield synthesis of complex gold nanostructures in a fungal system. J. Phys. Chem. C 111, 16858–16865.

Yang, L., Aguilar, Z.P., Qu, F., Xu, H., Xu, H., Wei, H., 2015. Enhanced antimicrobial activity of silver nanoparticles-*Lonicera Japonica* Thunb combo. IET Nanobiotechnol. 10, 28–32.

Zengin, G., Sarikurkcu, C., Gunes, E., Uysal, A., Ceylan, R., Uysal, S., Gungor, H., Aktumsek, A., 2015. Two *Ganoderma* species: profiling of phenolic compounds by HPLC–DAD, antioxidant, antimicrobial and inhibitory activities on key enzymes linked to diabetes mellitus, Alzheimer's disease and skin disorders. Food Func. 6, 2794–2802.

Zhou, Y., Kong, Y., Kundu, S., Cirillo, J.D., Liang, H., 2012. Antibacterial activities of gold and silver nanoparticles against *Escherichia coli* and bacillus Calmette-Guérin. J. Nanobiotechnol. 10, 19.